

Aurophilic Interactions from Wave Function, Symmetry-Adapted Perturbation Theory, and Rangehybrid Approaches

Ru-Fen Liu,[†] Christina A. Franzese,[‡] Ryan Malek,[‡] Piotr S. Żuchowski,[§] János G. Ángyán,^{*,†} Małgorzata M. Szczęśniak,^{*,‡} and Grzegorz Chałasiński^{‡,||}

[†]Crystallographie, Résonance Magnétique et Modélisations, Institut Jean Barriol, Nancy University and CNRS, F-54506 Vandœuvre-lès-Nancy, France

[‡]Department of Chemistry, Oakland University, Rochester, Michigan 48309, United States

[§]School of Chemistry, The University of Nottingham, Nottingham NG7 2RD, Great Britain

^{||}Faculty of Chemistry, University of Warsaw, Pasteura 1, 02-093 Warszawa, Poland

ABSTRACT: The aurophilic interaction is examined in three model systems $\text{Au}_2(^3\Sigma_g^+)$, $(\text{AuH})_2$, and $(\text{HAuPH}_3)_2$ which contain interactions of pairs of the Au centers in the oxidation state (I). Several methods are employed ranging from wave function theory-based (WFT) approaches to symmetry-adapted perturbation theory (SAPT) and range-separated hybrid (RSH) density functional theory (DFT) methods. The most promising and accurate approach consists of a combination of the DFT and WFT approaches in the RSH framework. In this combination the short-range DFT handles the slow convergence of the correlation cusp, whereas the long-range WFT is best suited for the long-range correlation. Of the three tested RSH DFT methods, the one which uses a short-range exchange functional based on the Ernzerhof–Perdew exchange hole model with a range-separation parameter of 0.4 bohr^{-1} seems to be the best candidate for treatment of gold. In combination with the long-range coupled cluster singles, doubles, and noniterative triples [CCSD(T)] treatment it places the strength of aurophilic bonding in $(\text{HAuPH}_3)_2$ at 5.7 kcal/mol at $R = 3.09 \text{ \AA}$. This value is somewhat larger than our best purely WFT result based on CCSD(T), 4.95 kcal/mol ($R = 3.1 \text{ \AA}$), and considerably smaller than the Hartree–Fock+dispersion value of 7.4 kcal/mol ($R = 2.9 \text{ \AA}$). The 5.7 kcal/mol estimate fits reasonably well within the prediction of the empirical relationship proposed by Schwerdtfeger et al. (*J. Am. Chem. Soc.* **1998**, *120*, 6587). A direct computation of dispersion energy, including exchange corrections, results in values of ca. -9 kcal/mol for $\text{Au}_2(^3\Sigma_g^+)$ and $(\text{AuH})_2$ and -13 kcal/mol for $(\text{HAuPH}_3)_2$ at the distance of a typical aurophilic bond, $R = 3.0 \text{ \AA}$.

I. INTRODUCTION

Experimental studies of two-coordinate gold compounds reveal structural motifs where Au(I) centers are in direct contact with each other but are not chemically bound. This provides the evidence for intermolecular bonding between seemingly closed-shell (5d)¹⁰ Au(I) cores known as aurophilic interactions.¹ The d¹⁰ subshells are spherically symmetric and exhibit valence repulsion; thus, the attractive interactions must originate, or so the explanation goes, from the dispersion effect, i.e., a nonlocal, dynamic correlation.^{2,3} Aurophilic interactions are comparable in strength to hydrogen bonding and play an important competing role in the assembly of gold compounds.¹ Other reasons for interest in these interactions include their relevance to the electronic structure of gold nanoparticles, where Au(I) cores provide the confining potential for a collective behavior of jellium electrons.⁴ Therefore, study of these interactions has wider implications for the coordination chemistry of gold, gold clusters, and gold nanoparticle–ligand interactions.

Previous computational studies of the aurophilic effect employed wave function theory (WFT) and density functional theory (DFT) based methodologies, as surveyed recently in exhaustive review papers.^{2,3} To our knowledge, no publication appeared on the use of recent rangehybrid methods for description of aurophilicity. Except for a very recent publication,⁵ aurophilic interactions have not been systematically studied by symmetry-adapted

perturbation theory (SAPT), which is a method intrinsically designed for intermolecular forces.

To summarize some highlights of previous studies, one should start from the work of Pyykkö and Zhao, who proposed a clever model for studying the aurophilic effect, $(\text{XAuPH}_3)_2$ ($X = \text{ligand}$) (in a gauche orientation), and first determined that the interaction between the Au(I) centers originated from electron correlation effects.⁶ An important finding of Pyykkö et al. was that in the Møller–Plesset (MP2), CCSD, and CCSD(T) series the correlation shows an oscillatory behavior. Therefore, the use of MP2 may overestimate interaction energies by as much as a factor of 2 compared with CCSD(T).⁷ The work of Magnko et al.⁸ on the same model $(\text{XAuPH}_3)_2$ ($X = \text{H, Cl}$) employed supermolecular, local MP2 (LMP2) calculations. From the analysis of LMP2 excitations the authors concluded that for the complex with $X = \text{H}$ about one-half of the post-Hartree–Fock (HF) attraction originated from dispersion-type excitations while the rest came from ionic contributions. Both post-HF contributions displayed distinctly different distance dependence. More recently, Pyykkö and Zaleski-Ejgierd estimated the basis set limit for the MP2 interaction⁹ in the same system. O’Grady and Kaltsoyannis¹⁰ carefully compared several WFT treatments

Received: April 8, 2011

Published: July 01, 2011

and made the first attempt to test DFT with the BP86 functional in the context of aurophilic (and metallophilic) interactions. They were surprised to observe that “DFT values are not significantly out of step with the ab initio results” although “the reasons why are not clear”. Assadollahzadeh and Schwerdtfeger¹¹ presented further comparisons of the BP86 DFT and WFT approaches for other ligands in the studies of the nonadditivity of aurophilic interactions.

Density functional theory in the Kohn–Sham formulation and with standard exchange–correlation functionals is able to provide a reliable description of short-range dynamic correlation effects, and in special circumstances it is able to mimic some amount of static correlation as well.¹² However, strongly non-local dynamic correlation effects, responsible for London dispersion forces, still remain a formidable challenge for DFT¹³ despite vigorous efforts to design new DFT-based methods, which are suited for this purpose. For aurophilic interactions, the words of Pyykkö, “No proof has been given that any supramolecular DFT treatment would reproduce the aurophilic attraction for a good physical reason”,³ remain certainly valid for all conventional local and semilocal functionals used in a simple Kohn–Sham framework. However, it might be worthwhile to revisit some aspects of Pyykkö’s statement in light of recent works aimed at including the London dispersion forces in DFT calculations. Extensively parametrized semiempirical functionals, like M05-2X¹⁴ and M06-2X¹⁵ of the Truhlar group, which proved to be extremely successful for a wide range of phenomena, including binding in van der Waals complexes around their equilibrium structures, fail to grasp physical origins of dispersion forces as reflected by the fact that the asymptotic $1/R^6$ decay of the potential energy is completely missed. Therefore, from our point of view, they are of rather limited interest. Promising new developments include the nonlocal vdW functionals,^{16,17} the a posteriori correction of the DFT total energy with $C_6 R^{-6}$ or higher-order atom–atom type corrections, exemplified by the work of Grimme,¹⁸ which in its more recent variant adjusts the atomic dispersion coefficient by an appropriate algorithm to the local bonding environment.¹⁹ Following different routes, the atomic dispersion coefficients can be made functionals of the density, as in the approach of Tkatchenko and Scheffler²⁰ or in the model of Becke and Johnson of the local properties of the exchange hole.²¹ Another type of recent development ensures the presence of dynamic correlation effects, responsible for London dispersion forces, by a generalization of the concept of hybrid functionals. In this category, one should mention the double-hybrid functionals with an explicit, usually empirically weighted MP2 contribution, such as B2LYP²² or XYG3,²³ and finally the combination of short-range DFT with long-range WFT treatment of the dynamical correlation in a range-separated hybrid framework.^{24–27} It is worth mentioning that several of these rangehybrid approaches have been used for a systematic study of the group 11 hydrides and halides.²⁸ Some of these different categories of functionals designed for dispersion forces have recently been compared and tested by Sherrill and co-workers.²⁹ We think that it is timely to explore the impact of some of these new advances on the understanding of aurophilic interactions.

In all previous works on aurophilic interactions (except for a very recent contribution⁵) their nature was inferred from supermolecular calculations, i.e., from such observations as the repulsive HF potential and the R^{-6} asymptotic behavior of the supermolecular interaction energy upon inclusion of correlation.³

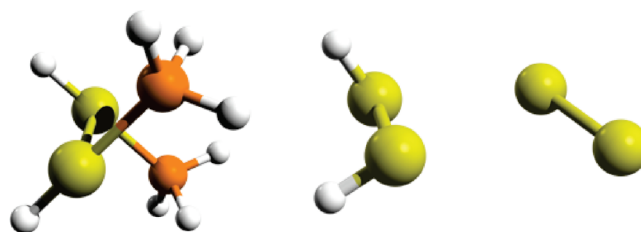


Figure 1. Geometrical configurations of three model aurophilic compounds.

One of the goals of the present paper is to determine the nature of the interaction between the two Au(I) centers embedded in a molecular framework by direct application of the perturbation theory approach. The Au(I)—Au(I) interacting unit will be included in three model systems of decreasing complexity. We begin with the same model system as that used in the work of Pyykkö and Zhao⁶—a dimer of the two-coordinate Au species: HAuPH_3 in a gauche configuration (i.e., with a dihedral angle of 90° , which allows for minimization of electrostatic forces by ensuring a vanishing dipole–dipole interaction). Next, the two PH_3 ligands are removed and one has $(\text{AuH})_2$ in a gauche conformation. A thallium analog of this model was used by Schwerdtfeger in 1991³⁰ as a model system for $\text{Tl(I)}-\text{Tl(I)}$ thalophilic interactions to show that the attraction is essentially a correlation effect. Next, the H atoms are removed, leaving Au_2 in the $^3\Sigma_u^+$ state (see Figure 1).

A broader objective of the present study is to demonstrate that the challenges of aurophilic interactions, which are indeed considerable, can be met using the methodologies based on the concept of range separation that combine the advantages of DFT for short-range electron–electron interactions with the long-range capabilities of WFT methods. The main advantage of WFT methods is that they allow for a clear-cut identification of dispersion forces as a post-HF correlation effect. While one can be sure that at the HF level the London dispersion forces cannot be present, such clear guidance is absent in Kohn–Sham calculations. On one hand, it has been observed that numerous exchange–correlation (xc) functionals lead to sometimes quite reasonable attractive wells on potential energy curves even for the simplest, fully dispersion-bound systems, such as rare gas binary complexes. Typically, LDA and GGA functionals, usually based on a Perdew-type exchange functional (e.g., PBE, PW91), which satisfy the Lieb–Oxford bound³¹ locally, fall in this category. On the other hand, in functionals based on an exchange component as developed by Becke, no binding is observed in the above-mentioned category of dispersion-bound complexes; on the contrary, the potential curves are often significantly more repulsive than the HF ones.³²

How does one choose a functional which provides reasonable reference energy for explicit, physically sound dispersion corrections? One strategy consists in tailoring an xc functional to reproduce as well as possible the genuinely dispersion-free HF potential curve. Several groups have shown recently the feasibility of this approach.^{33,34} An alternative strategy is based on the use of mutually polarized Kohn–Sham densities of the monomers and an explicit calculation of the intermolecular Coulomb and exchange effects.³⁵ The spurious overpolarization of the monomers has been avoided by a Pauli–blockade method,³⁶ leading to dispersion-free total energy. Finally, similar results can be obtained in the rangehybrid scheme, where long-range

(predominantly) intermolecular electron–electron (e–e) interactions are treated at the HF level while short-range (intramolecular) e–e interactions are handled by a short-range xc functional. Such hybrid calculations lead to essentially dispersion-free total energies, as first shown by the group of Hirao,³⁷ constituting a convenient starting point for long-range WFT correlation treatments of dispersion effects.

II. METHOD AND COMPUTATIONAL DETAILS

The gold atoms are described using the 19-electron, small-core (1s–4f), relativistic effective core potential (ECP) of Figgen et al.³⁸ ECP is combined with the augmented correlation-consistent basis set of triple- ζ quality (unless stated otherwise) recently optimized by Peterson and Puzarini (aug-cc-pVTZ-PP), which includes orbitals up to the g symmetry.³⁹ The remaining atoms are described by the aug-cc-pVTZ basis set.⁴⁰

The supermolecular calculations are performed at several post-HF levels of theory up to CCSD(T)⁴¹ defining the interaction energy as

$$E_{\text{int}}^{\text{X}} = E_{\text{dimer}}^{\text{X}} - 2E_{\text{monomer}}^{\text{X}}, \text{ where } \text{X} = \text{HF}, \\ \text{HF} + \text{MP2}, \text{HF} + \text{CCSD}, \text{HF} + \text{CCSD(T)}$$

where the monomer contributions are calculated in the basis set of the whole dimer. For direct comparison with the dispersion energy we also use the quantity $E_{\text{int}}^{\text{corr}}$ which is the correlation contribution to the interaction energy at a given level and defined as the difference between $E_{\text{int}}^{\text{X}}$ and $E_{\text{int}}^{\text{HF}}$. In the correlated calculations the outer-core $5s^2 5p^6$ electrons were active.

The calculations of dispersion energy and its exchange counterpart employ two variants of symmetry adapted perturbation theory. For $^3\text{Au}_2$ WFT open-shell symmetry adapted perturbation theory [SAPT(WFT)] is used.⁴² The dispersion energy is obtained from the time-dependent (TD) coupled HF theory as described in ref 43 and henceforth denoted $E_{\text{disp}}^{(2)}(\text{CHF})$, and its exchange counterpart is $E_{\text{exdisp}}^{(2)}(\text{CHF})$. For the remaining dimers, which are closed shell, SAPT theory based on the DFT description of monomers⁴⁴ is used as implemented in MOLPRO.⁴⁵ According to SAPT(DFT), the total interaction energy through the second-order perturbation theory, DSAPT[2], is expressed as the following sum of the electrostatic (es), induction (ind), and dispersion (disp) terms as well as their respective exchange counterparts

$$\text{DSAPT}[2] = E_{\text{es}}^{(1)} + E_{\text{exch}}^{(1)} + E_{\text{ind}}^{(2)} + E_{\text{exind}}^{(2)} + E_{\text{disp}}^{(2)} + E_{\text{exdisp}}^{(2)} \quad (1)$$

where the perturbation terms are obtained from Kohn–Sham (KS) orbitals. The induction and dispersion terms as well as their exchange counterparts are obtained from the coupled KS (CKS) approach (see refs 46 and 47 for details). The dispersion and exchange–dispersion terms will henceforth be denoted $E_{\text{disp}}^{(2)}(\text{CKS})$ and $E_{\text{exdisp}}^{(2)}(\text{CKS})$, respectively. Additionally, a residual HF term, δ_{HF} , is defined as a supplement to eq 1 with higher order terms and other residual effects taken from the HF level

$$\delta_{\text{HF}} = E_{\text{int}}^{\text{HF}} - E_{\text{es}}^{(1)} - E_{\text{exch}}^{(1)} - E_{\text{ind}}^{(2)}(\text{CHF}) - E_{\text{exind}}^{(2)}(\text{CHF}) \quad (2)$$

where the perturbation terms subtracted from the supermolecular HF interaction energy are all evaluated from the HF orbitals. The KS orbitals for the SAPT(DFT) calculations are obtained using the asymptotically corrected⁴⁸ PBE0 functional.⁴⁹

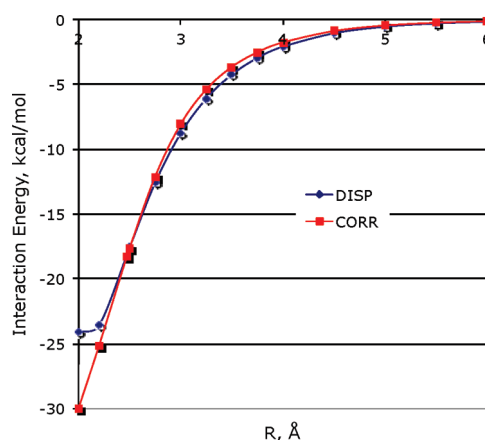


Figure 2. Comparison between the total dispersion energy $E_{\text{disp}}^{(2)}(\text{CHF}) + E_{\text{exdisp}}^{(2)}(\text{CHF})$ (denoted DISP) of $^3\text{Au}_2$ and the correlation contribution to the interaction energy at the CCSD(T) level of theory (CORR).

Range-separated hybrid (RSH) calculations have been performed with a range-separation parameter μ of 0.5 and 0.4 bohr^{−1} for sr-LDA and sr-PBE functionals, respectively. Several independent studies indicated these values as optimal.^{50–52} The short-range LDA and two flavors of short-range PBE xc functionals have been explored in the present work. The sr-LDA functional is composed of the short-range LDA exchange⁵³ and the complementary short-range correlation derived from Quantum Monte Carlo simulations on the long-range interacting homogeneous electron gas.⁵⁴ The sr-PBE functionals differ only in their exchange components. One of the variants is based on the form suggested by Toulouse et al.⁵⁵ and extended by Goll et al.^{56,57} and keeps the same form as the original PBE functional but introduces a μ dependence of the parameters. The second type of sr exchange functional is constructed from an analytical model of the PBE exchange hole, developed by Ernzerhof and Perdew⁵⁸ (referred to here as PBE-EP), which is integrated with the short-range interaction function, $\text{erfc}(\mu r)/r$ (see also ref 59). This approach is analogous to the method followed in the construction of the HSE functional,⁶⁰ the main difference being that the role of the short and long range is inverted. The sr-PBE correlation functional used here has been described in ref 57. The applied rangehybrid methods will be designated by the following acronyms: sr-{LDA,PBE,PBE-EP}+lr-{MP2,CCSD,CCSD(T)}. The basis set is the same augmented valence triple- ζ quality as for the full-range correlated WFT and SAPT calculations, with the only difference being that it is not augmented on the phosphine H atoms.

The geometrical parameters are as follows. In gauche $(\text{AuH})_2$ complex $r(\text{Au}–\text{H}) = 1.524 \text{ Å}$. In $(\text{HAuPH}_3)_2$ we use the same dimer configuration as in ref 8. In the WFT and SAPT calculations the intramonomer HAuPH_3 geometrical parameters were taken from ref 8 ($r(\text{Au}–\text{P}) = 2.385 \text{ Å}$, $r(\text{Au}–\text{H}) = 1.606 \text{ Å}$, $r(\text{P}–\text{H}) = 1.416 \text{ Å}$, $\angle(\text{H}–\text{P}–\text{Au}) = 118.5^\circ$), whereas in the rangehybrid calculations these parameters were optimized at the CCSD(T) level of theory ($r(\text{Au}–\text{P}) = 2.325 \text{ Å}$, $r(\text{Au}–\text{H}) = 1.598 \text{ Å}$, $r(\text{P}–\text{H}) = 1.407 \text{ Å}$, $\angle(\text{H}–\text{P}–\text{Au}) = 119^\circ$).⁶² The basis sets in these geometry optimizations were ECP-VTZ for Au and VTZ (without augmentation functions) on the P and H atoms. The coordinate $R(\text{Au}–\text{Au})$ was varied keeping the monomer geometries unchanged.

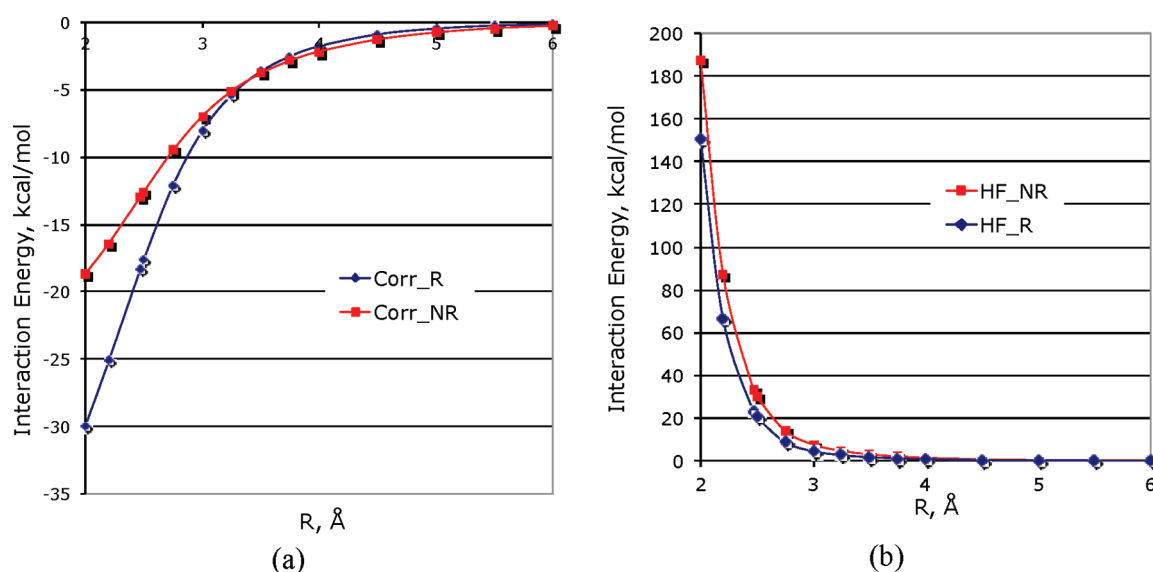


Figure 3. Comparison of “nonrelativistic” (NR) and “relativistic” (R) treatment of the interaction energy in $^3\text{Au}_2$: (a) correlation CCSD(T) contribution to the interaction energy and (b) uncorrelated HF component. For definitions see the text.

III. RESULTS AND DISCUSSION

1. WFT and SAPT Methods. *a. Dispersion Energy in $\text{Au}_2(^3\Sigma_u^+)$.* It is convenient to begin our discussion with the interaction between Au atoms in the $\text{Au}_2(^3\Sigma_u^+)$ state. The open-shell calculations in this section are performed using spin-restricted coupled cluster formalism and spin-unrestricted formalism in the SAPT dispersion calculations (unless stated otherwise).

In the ground state Au_2 is covalently bound by a single σ bond formed by two 6s electrons. In $^3\Sigma_u^+$ state the molecule is bound by long-range forces. The key difference between the two states is the exchange energy, which distinguishes the singlet from the triplet state. The ground state $\text{Au}_2(^1\Sigma_g^+)$ has been carefully benchmarked by Peterson and Puzzarini³⁹ using CCSD(T). Their calculation, which included relativistic effects, basis set limit estimation, and core–valence correlation, yielded a well depth of 53.2 kcal/mol at $R_e = 2.47$ Å. Our present treatment places the well depth of the ground state some 7% above their value. For the $\text{Au}_2(^3\Sigma_u^+)$ state we obtain a well depth of 3.698 kcal/mol at the roughly optimized R_e of 2.924 Å at the UCCSD(T). A recent, more saturated CCSD(T) result for D_e for this complex is reported to be 4.3 kcal/mol.⁶³

In our calculations of the CHF dispersion energy, which is known to be more basis-set dependent than the CKS variants,⁶⁴ we employ a slightly larger basis set (aug-cc-pVQZ-PP from which the more compact g and h orbitals were removed) augmented by a bond function (3s, 3p, 3d, 3f).

A comparison between the sum of $E_{\text{disp}}^{(2)}(\text{CHF}) + E_{\text{exdisp}}^{(2)}(\text{CHF})$ of $^3\text{Au}_2$ and the correlation contribution to this interaction $E_{\text{int}}^{\text{CCSD(T)}}$ is presented in Figure 2.

One can see that the two quantities agree extremely well in the wide range of distances. Two values of dispersion energy are particularly noteworthy. Around the van der Waals minimum of $^3\text{Au}_2$ ($R = 3$ Å) the dispersion effect amounts to -8.8 kcal/mol with $E_{\text{disp}}^{(2)}(\text{CHF}) = -12.36$ kcal/mol and $E_{\text{exdisp}}^{(2)}(\text{CHF}) = 3.57$ kcal/mol. Around the chemically bound minimum $^1\text{Au}_2$ ($R = 2.47$ Å) the total dispersion effect amounts to -18.22 kcal/mol out of which the dispersion is -29.75 kcal/mol and the exchange

dispersion is 11.53 kcal/mol. The C_6 dispersion coefficient fit to the long-range tail of the RHF-UCCSD(T) correlation interaction energy of $^3\text{Au}_2$ amounts to 345 au. This value increases by 4.5% upon freezing the 5s, 5p electrons in the calculations.

Next, we examine the effect of the scalar relativity on the dispersion interaction and more precisely on the correlation contribution to the $^3\text{Au}_2$ bonding. The relativistic effects lower the static dipole polarizability of Au from 64 to about 36 au.⁶⁵ They also lead to the doubling of the electron affinity of Au (from 1.283 to 2.295 eV) and to the increase of the ionization potential by some 2 eV (see Table 3 in ref 3). In gold–ligand interactions Au– PH_3 these effects result in a “relativistic bond” as described by Granatier et al.⁶⁶ Our present comparison is indirect and qualitative in nature and involves the following strategy: For the “nonrelativistic” treatment we perform all-electron calculations, without the Douglas–Kroll option, and with the fully nonrelativistic basis set named Hy-PolX.⁶⁷ The “relativistic” calculation employs the above-mentioned relativistic ECP with aug-cc-pVTZ-PP, which contains a similar number and type of polarization functions as Hy-PolX. To ensure that the same number of electrons is correlated in both calculations, the former keeps 68 electrons on each Au in the core while the latter keeps 8 electrons on each Au in the core. The result of this comparison is shown in Figure 3.

It appears that in the long range the “nonrelativistic” curve is slightly more attractive, consistent with the larger nonrelativistic static polarizability, if London’s model of dispersion is to be followed. In the short range the “relativistic” curve is more attractive, reflecting the larger ionization potential at the relativistic level. It is also interesting that the curves cross each other around 3.2 Å. Thus, at shorter distances, relativistic effects slightly strengthen and at longer distances slightly weaken the correlation interaction in $^3\text{Au}_2$. However, the most significant changes between the two approaches appear (not unexpectedly) at the HF level of theory. As seen in Figure 3b, the relativistic effects shift the repulsive wall toward shorter distances, enabling the atoms to approach closer and thus benefitting from a stronger dispersion attraction.

Table 1. Three-Body (3-b) Contributions in $^4\text{Au}_3$ from Restricted Open-Shell CCSD(T) Calculations (in kcal/mol)^a

geometry	$E_{\text{int}}(\text{abc})$	$E_{3-\text{b}}(\text{HF})$	$E_{3-\text{b}}(\text{corr})$
D_{3h}	−11.49	−2.33	0.51
$D_{\infty h}$	−6.30	0.41	−0.21

^a The three-body term is partitioned into the HF and correlation contributions.

Table 2. Comparison of $^3\text{Au}_2$, $(\text{AuH})_2$, and $(\text{HAuPH}_3)_2$ Interaction Energies at $R = 3 \text{ \AA}$ (in kcal/mol)^a

term	$^3\text{Au}_2$	$(\text{AuH})_2$	$(\text{HAuPH}_3)_2$
HF	4.43	3.21	5.63
HF+CCSD(T)	−3.64	−2.93	−4.83
HF+CCSD	−2.12	−1.75	−2.82
HF+MP2	−5.05	−5.73	−8.92
HF+Disp	−4.36	−5.94	−7.40
$E_{\text{disp+ex}}^{(2)}(\text{CKS})$	−8.80 ^b	−9.06	−13.02 (−12.28)
$E_{\text{disp+ex}}^{(2)}(\text{UCKS})$		−19.07	−27.01 (−17.47)

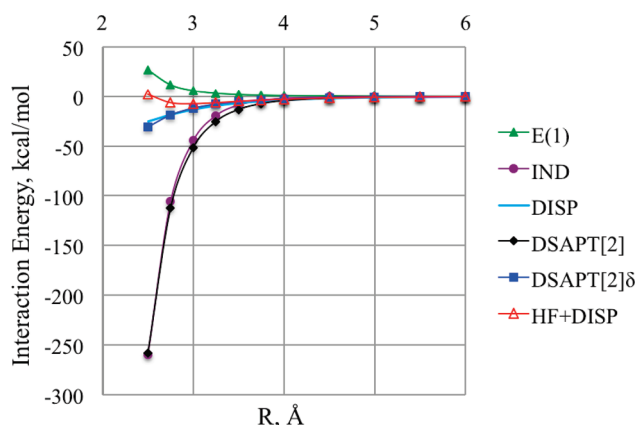
^a The values in parentheses for $(\text{HAuPH}_3)_2$ correspond to $E_{\text{disp+ex}}^{(2)}$ from CHF and UCHF calculations, respectively. ^b from the CHF calculations.

Finally, it is also possible to evaluate the magnitude and sign of the three-body terms in the interaction of three Au atoms. To this end, we choose the high-spin, quartet Au_3 for which the restricted open-shell CCSD(T) calculations are performed. The results are shown in Table 1.

$E_{\text{int}}(\text{abc})$ denotes the entire trimer interaction energy (i.e., both two-body and three-body terms). Assuming that the correlation contribution to the interaction energy consists mainly of the dispersion energy (as shown above in the two-body case), we observe that the three-body dispersion interaction is positive in the equilateral triangle configuration and slightly negative in the linear configuration, which is consistent with the Axilrod–Teller–Muto angular dependence of the dispersion interactions as well as with our previous diagrammatic analysis of the n -body contributions to the supermolecular MP perturbation theory interaction energies.⁶⁸ One can also notice that the nonadditivity of the HF interaction energy has a opposite sign as it results from the first-order exchange three-body term (see a similar behavior for other metals from Ia and Ib groups⁶⁹).

b. $(\text{AuH})_2$. A comparison between the results for $^3\text{Au}_2$, $(\text{AuH})_2$, and $(\text{HAuPH}_3)_2$ is shown in Table 2. Let us focus on the first two, leaving $(\text{HAuPH}_3)_2$ for later discussion. The calculations for $(\text{AuH})_2$ are performed for the orientation of the monomers shown in Figure 1 (C_2 point group). The supermolecular dimer CCSD(T) calculations indicate that there may be some multi-configurational character in the reference function, namely, rather large T1 (0.03) and D1 (0.1) diagnostic^{70,71} values have been found. Indeed, the EOM-CCSD calculations show that there are two low-lying singly excited states ^1B and ^1A at 2.97 and 3.13 eV, respectively, at $R = 3.0 \text{ \AA}$. Nevertheless, the CCSD(T) calculations provide results consistent with those for $^3\text{Au}_2$ and yield a CCSD(T) interaction curve with the minimum at $R(\text{Au}–\text{Au}) = 3.09 \text{ \AA}$ with a well depth of 3.03 kcal/mol.

Both $^3\text{Au}_2$ and $(\text{AuH})_2$ have purely repulsive HF potential curves, and they are bound only upon inclusion of correlation effects. Both complexes have further similar characteristics: they are relatively weakly bound by about −3.6 and −2.93 kcal/mol,

**Figure 4.** Radial dependence of the interaction energy terms in $(\text{HAuPH}_3)_2$ from SAPT(DFT). $E(1)$ denotes the sum of the electrostatic and exchange energy, IND denotes the sum the CKS induction and exchange-induction terms, DISP denotes the sum of the CKS dispersion and exchange-dispersion terms, $\text{DSAPT}[2]$ denotes the sum of the SAPT(DFT) terms through the second order, see eq 1, and $\text{DSAPT}[2]\delta$ includes also the residual δ_{HF} term of eq 2.

respectively, and their total dispersion effect (including exchange) is very similar, −8.8 vs −9.1 kcal/mol, respectively. It is particularly noteworthy that uncoupled KS dispersion energy is severely overestimated in magnitude. Compared to HF+CCSD(T), HF+MP2 leads to a stronger binding. Also shown is the HF+Disp approximation, which combines HF with the coupled dispersion and exchange–dispersion terms. In $^3\text{Au}_2$ this approximation gives values in reasonable agreement with HF+CCSD(T) as discussed in the previous section. In the case of $(\text{AuH})_2$ it exceeds HF+CCSD(T) by a factor of 2.

c. $(\text{HAuPH}_3)_2$. The supermolecular HF+CCSD(T) calculations for this dimer, in the geometry shown in Figure 1, yield a well depth of 4.95 kcal/mol at around $R(\text{Au}–\text{Au}) = 3.1 \text{ \AA}$. In this value the effects of outer-core correlation (i.e., 5s and 5p electrons in Au) contribute only 0.2 kcal/mol toward the stabilization. Incidentally, both types of diagnostics, T1 and D1, are in the normal range, indicating that the single-reference character improves upon addition of the PH_3 ligands. However, this result obtained in aug-cc-pVTZ is probably far from basis set saturation. The HF interaction energy results in a purely repulsive potential curve. SAPT(DFT) values of dispersion energy terms $E_{\text{disp}}^{(2)}(\text{CKS})$ and $E_{\text{exdisp}}^{(2)}(\text{CKS})$ are also shown. In addition, we also list corresponding values of dispersion energy calculated using the CHF and UCHF approach, $E_{\text{disp+ex}}^{(2)}(\text{CHF})$ and $E_{\text{disp+ex}}^{(2)}(\text{UCHF})$, respectively. The other SAPT(DFT) components are not shown because the theory appears to diverge for aurophilic interactions.

Figure 4 shows the R dependence of the SAPT(DFT) contributions for $(\text{HAuPH}_3)_2$. $\text{DSAPT}[2]$, the sum of all the terms through the second order (see eq 1), is dominated by the induction effects and falls precipitously for shorter distances without any minimum. Adding the residual HF term δ_{HF} (eq 2) as suggested in the instances of using ECP (see refs 72 and 73) also fails to produce the minimum (see $\text{DSAPT}[2]\delta$ curve). One should add that δ_{HF} , which is strongly repulsive, eludes physical justification. By contrast, HF+Disp displays a minimum with reasonable position and depth (see Figure 4).

The causes of the SAPT divergence are related to the overestimated induction energy (−131 kcal/mol at $R = 3.0 \text{ \AA}$!), which cannot be properly constrained by the exchange effects

(see Figure 4). The approximate treatment of the exchange interactions with the partner's core as a result of using the ECP (see ref 72) is a contributing factor but not the cause of it. Broadly speaking, it is the fundamental inseparability of the induction and exchange, which is the root of this problem.⁷⁴ It should be stressed that the calculated values of the dispersion and exchange dispersion terms are sound.

The equilibrium results obtained at various levels of theory are shown in Table 2, where they can be compared with both $(\text{AuH})_2$ and $^3\text{Au}_2$. The $(\text{HAuPH}_3)_2$ dimer is more strongly bound than the other Au-containing systems, but the pattern is similar: the dimer is unbound at the HF level of theory; HF+MP2 overestimates the binding compared to HF+CCSD(T) to an even greater degree. The same is true of the HF+Disp approximation. The strengthening of the aurophilic bonding upon addition of the PH_3 group to AuH can be explained by a subtle balance between the first-order repulsion and dispersion attraction. For example, at $R = 3.0 \text{ \AA}$ addition of PH_3 results in the 2.4 kcal/mol net gain in the first-order interaction ($E_{\text{es}}^{(1)} + E_{\text{exch}}^{(1)}$), which almost exactly accounts for the change in the HF term (Table 2). Simultaneously, adding the ligands leads to enhanced net dispersion ($E_{\text{disp}}^{(2)} + E_{\text{exdisp}}^{(2)}$) stabilization of -4 kcal/mol .

In aurophilic interactions one is faced with a number of unpleasant realities: (i) the cluster expansion converges slowly as evidenced by the large contribution from the triples; (ii) the HF+Disp approximation overestimates the interaction as compared to HF+CCSD(T). Furthermore, as seen in Table 2, the UCHF dispersion energy is too large in magnitude compared to both CHF and CKS (although not as outrageously so as UCKS). Since the UCHF type of dispersion resides implicitly in the supermolecular MP2 interaction contribution,^{75,76} HF+MP2 should also lead to overbinding. Finally, it is not possible to substitute the HF interaction for another “dispersionless” approach based on SAPT(DFT) because the latter is divergent and the quality of its components cannot be ascertained.

2. Range-Separated DFT + WFT Approaches for Aurophilic Interactions. The combined sr-DFT + lr-WFT approaches have proven very successful in such challenging systems as rare gas dimers^{56,77} and alkaline earth dimers.^{78–80} Therefore, it is interesting to test them in the circumstance of the aurophilic bond. Such approaches are predicated on the range separation of the e–e interactions,^{24,53,78,81–83} where the short range is described within the DFT theory and the long range, nonlocal correlation is obtained from the WFT methodology. The calculations in this section are performed in a slightly different monomer geometry of HAuPH_3 (see section II), which has a negligible effect on the interaction energy.⁶²

The first emerging question is how to select the sr-DFT containing only the short-range correlation effects, i.e., which is expected to be essentially dispersion free. It is difficult to predict how the dispersion-free potential should appear for $\text{Au(I)}-\text{Au(I)}$ and by what criteria it should be judged. Unlike for rare-gas dimers where one is certain that such potential should be repulsive there is no such certitude in the present case, especially in light of the findings of refs 8 and 84 that have identified the nondispersion, post-HF ionic contributions to the aurophilic bond.

Figure 5a and 5b presents the sr-DFT potentials for $(\text{AuH})_2$ (Figure 5a) and $(\text{HAuPH}_3)_2$ (Figure 5b) obtained with the following range-separated functionals described in section II: sr-LDA ($\mu = 0.5$), sr-PBE ($\mu = 0.4$), and sr-PBE-EP ($\mu = 0.4$).

The results show that sr-PBE-EP is the least attractive of the three sr-DFT options for both systems, although it is much less

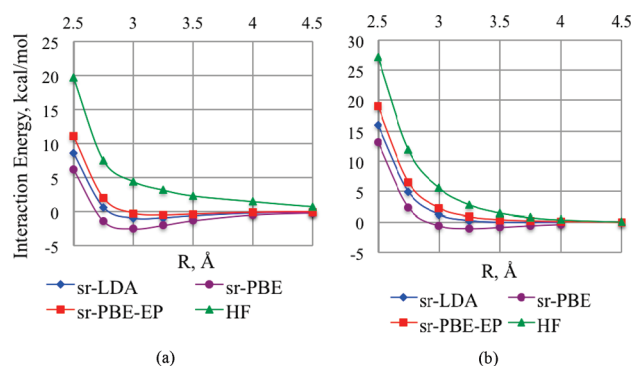


Figure 5. Comparison of sr-LDA, sr-PBE, and sr-PBE-EP potentials for (a) $(\text{AuH})_2$ and (b) $(\text{HAuPH}_3)_2$.

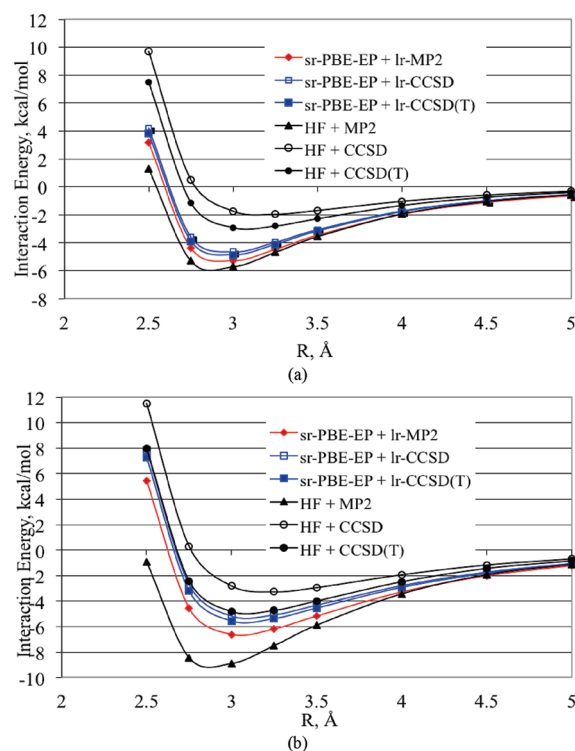


Figure 6. Comparison between sr-DFT + lr-WFT and full-range WFT approaches for (a) $(\text{AuH})_2$ and (b) $(\text{HAuPH}_3)_2$.

so than HF. sr-PBE is the most attractive of the three, whereas sr-LDA closely follows sr-PBE-EP. One can notice that even sr-PBE-EP and sr-LDA are slightly attractive for $(\text{AuH})_2$. However, the interaction between two AuH has some multiconfigurational character (see section b), which could manifest itself as short-range correlation effects (such as ionic contributions observed by Magnko et al.⁸)

In the next step the sr-DFT orbitals are used in the MP2, CCSD, and CCSD(T) calculations, resulting in lr-MP2, lr-CCSD, and lr-CCSD(T), which are added to the sr-DFT part. These are compared with the “full-range” WFT approaches HF+MP2, HF+CCSD, and HF+CCSD(T). The comparison is shown in Figure 6a for $(\text{AuH})_2$ and Figure 6b for $(\text{HAuPH}_3)_2$.

We observed before (see Table 2) that in full-range coupled cluster treatment the role of triples was overwhelming: 40% of the well depth in $(\text{AuH})_2$ and 42% in $(\text{HAuPH}_3)_2$. Furthermore,

Table 3. Energy Minimum Parameters of the (AuH)₂ and (HAuPH₃)₂ Dimers Obtained with Different Levels of Theory

theory	(AuH) ₂		(HAuPH ₃) ₂	
	E(min), kcal/mol	R(min), Å	E(min), kcal/mol	R(min), Å
HF+MP2	−6.01	2.89	−9.15	2.91
HF+CCSD	−2.04	3.16	−3.28	3.25
HF+CCSD(T)	−3.03	3.09	−4.95	3.11
HF+Disp	−6.04	2.91	−7.39	3.00
sr-PBE-EP	−0.52	3.18	−0.01	4.99
sr-PBE-EP + lr-MP2	−5.42	2.92	−6.68	3.06
sr-PBE-EP + lr-CCSD	−4.75	2.93	−5.37	3.10
sr-PBE-EP + lr-CCSD(T)	−5.01	2.93	−5.72	3.09
sr-LDA	−1.08	3.10	−0.04	3.58
sr-LDA + lr-MP2	−8.03	2.84	−9.84	2.89
sr-LDA + lr-CCSD	−6.38	2.87	−7.14	2.97
sr-LDA + lr-CCSD(T)	−6.84	2.86	−7.79	2.95
sr-PBE	−2.55	2.95	−1.05	3.20
sr-PBE + lr-MP2	−8.23	2.85	−9.86	2.90
sr-PBE + lr-CCSD	−7.51	2.86	−8.28	2.93
sr-PBE + lr-CCSD(T)	−7.80	2.86	−8.71	2.92

HF+MP2 overestimated the well depth of both complexes by nearly 2-fold. By contrast, our best candidate for dispersion-free rangehybrid, sr-PBE-EP, in combination with lr-WFT shows to be a quickly convergent treatment of electron correlation. Specifically, in both complexes, the sensitivity to triples has practically disappeared. The performance of lr-MP2 also appears to be much improved compared to the full-range approach, particularly for (HAuPH₃)₂. For (AuH)₂ the three range-separated sr-DFT + lr-WFT potentials which run very close to each other are considerably deeper than HF+CCSD(T). This again may be related to the fact that already the dispersion-free sr-PBE-EP is slightly attractive. Overall, the results show that the sr-PBE-EP rangehybrid combined with lr-WFT provides an excellent description of auophilic interactions. To see how the remaining sr-DFT approaches behave in combination with lr-WFT we summarize the equilibrium well-depth parameters in Table 3.

The sr-LDA approach combined with lr-WFT leads to deeper potential wells (by up to 2 kcal/mol for lr-CCSD/CCSD(T) and 3 kcal/mol for lr-MP2) with minima shifted toward shorter distances. For sr-PBE combined with lr-WFT the deepening is even more pronounced. Still the effect of triples in lr-CCSD(T) is quite small, on the order of 0.5 kcal/mol or less. Interestingly, it is not the lr-correlation which differentiates between the potentials. For (AuH)₂, the lr-CCSD contribution at R = 3.0 Å is almost the same if obtained from the sr-PBE-EP or sr-PBE orbitals, namely, −7.46 vs −7.57 kcal/mol, respectively. The differences reside in the sr-DFT, i.e., the putative dispersion-free part of the interaction. Let us also mention that the lr-CCSD contribution obtained from the sr-LDA orbitals amounts to −8.35 kcal/mol and that from the HF orbitals amounts to −8.45 kcal/mol. Finally, the lr-CCSD(T) calculations lead to the dramatically improved T1 and D1 diagnostics. For example, the sr-PBE-EP + lr-CCSD(T) calculations give at R = 3 Å the T1/D1 diagnostics of 0.0146/0.04689 and 0.0102/0.0339 for (AuH)₂ and (HAuPH₃)₂, respectively.

From the computational point of view, there is at present no particular time advantage of the sr-DFT + lr-WFT approach if one compares the calculations in the same basis set. However, since the basis set gets saturated much faster, a “converged” result is much cheaper to obtain.

IV. CONCLUSIONS

Auophilic interactions present a formidable challenge for computational treatments in that they include a large number of strongly correlated, relativistically contracted electrons. We explored a number of possible treatments for these interactions, which include symmetry-adapted perturbation theory, supermolecular full-range WFT methods, and the hybrid sr-DFT + lr-WFT approaches based on the concept of range separation.

SAPT(DFT) leads to a divergent description of these interactions due in large part to the spurious overpolarization of monomers which cannot be constrained by the exchange. A contributing factor is the use of the effective core potentials for the Au centers. The important SAPT(DFT) terms that appear to be unaffected are the dispersion and exchange–dispersion terms. This fact can be traced to the dispersion energy being related to the *two-electron* part of the intermolecular interaction operator as first noted in ref 72. When combined with the HF interaction energy, HF+Disp provides a reasonable approximation for ³Au₂ but becomes erratic for (AuH)₂ and (HAuPH₃)₂, presumably due to the larger role of the neglected intramonomer correlation. The dispersion attraction of two Au atoms is increased at long intersystem distances and reduced in the short range by inclusion of relativistic effects. These changes are consistent with the effects of relativity on the polarizability and ionization potential of Au. However, the strongest effect relativity exerts on the HF interaction potential, causing the shift of the repulsive wall toward shorter distances.

Of the full-range WFT approaches examined in this work, HF + MP2 leads to a significant overbinding because of a considerable overestimation of the dispersion energy by the UCHF approximation for auophilic interactions, as demonstrated in this work. The results of the HF+CCSD and HF+CCSD(T) calculations point to a significant role of triples. This indicates that to saturate correlation effects it may be necessary to include in the cluster expansion not only the iterative triple excitations but also the quadruples.

By contrast, the range-separated sr-DFT + lr-WFT approaches examined in this work show a much weaker dependence on the triple excitations as seen by the small difference between lr-CCSD and lr-CCSD(T) contributions. One plausible explanation is that the triple excitations are more important in the short range of the e–e interactions, but their contribution to the long range is smaller. In the combined sr-DFT + lr-WFT approach these short-range interactions are efficiently accounted for by a sr-DFT component.

The sr-DFT approach offers the added benefit of serving as a dispersion-free approximation—the DFT analog of the HF interaction energy. Of the three candidates examined here the sr-PBE-EP functional with a range-separation parameter of 0.4 appears to fit the characteristics of such an approximation for gold. We base this determination on the values of the sr-PBE-EP + lr-CCSD(T) interaction energies for (AuH)₂ and (HAuPH₃)₂, which appear to be the most sensible. The sr-PBE-EP+lr-CCSD(T) approach places the strength of auophilic interaction in the (HAuPH₃)₂ gauche dimer of the two unrelaxed monomers at

5.7 kcal/mol at $R = 3.09 \text{ \AA}$. This value is somewhat larger than the HF+CCSD(T) one of 4.95 kcal/mol ($R = 3.1 \text{ \AA}$) and considerably smaller than the HF+Disp value of 7.4 kcal/mol ($R = 2.9 \text{ \AA}$). The 5.7 kcal/mol estimate fits reasonably well within the prediction of the empirical relationship proposed by Schwerdtfeger et al.,⁸⁵ which gives ca. 6 kcal/mol at this distance.

The aurophilic interactions in $\text{Au}_2(^3\Sigma_g^+)$ and $(\text{AuH})_2$ models are very similar (-3.6 vs -2.9 kcal/mol). Addition of the PH_3 ligands to $(\text{AuH})_2$ results in a dramatic increase in the dispersion stabilization by 4 kcal/mol, which is counterbalanced by a 2.4 kcal/mol net increase in the first-order repulsion in the minimum region.

AUTHOR INFORMATION

Corresponding Author

*E-mail: Janos.Angyan@crm2.uhp-nancy.fr (J.G.A.), bryant@oakland.edu (M.M.S.).

ACKNOWLEDGMENT

This work was supported by the Agence Nationale de Recherche (France) in the framework of the project Metal–Metal (ANR-06-BLAN-0410), by the U.S. National Science Foundation (Grant No. CHE-0719260), and by the Polish Ministry of Science and Higher Education (Grant N N204 248440).

REFERENCES

- Schmidbaur, H.; Schier, A. *Chem. Soc. Rev.* **2008**, 37, 1931.
- Pyykkö, P. *Angew. Chem., Int. Ed.* **2004**, 43, 4412.
- Pyykkö, P. *Chem. Soc. Rev.* **2008**, 37, 1967.
- Walter, M.; Akola, J.; Lopez-Acevedo, O.; Jadzinsky, P. D.; Calero, G.; Ackerson, C. J.; Whetten, R. L.; Gronbeck, H.; Hakkinen, H. *Proc. Natl. Acad. Sci. U.S.A.* **2008**, 105, 9157.
- Muniz, J.; Wang, C.; Pyykkö, P. *Chem.—Eur. J.* **2011**, 17, 368.
- Pyykkö, P.; Zhao, Y. F. *Angew. Chem., Int. Ed. Engl.* **1991**, 30, 604.
- Pyykkö, P.; Runeberg, N.; Mendizabal, F. *Chem.—Eur. J.* **1997**, 3, 1451.
- Magnko, L.; Schweizer, M.; Rauhat, G.; Schutz, M.; Stoll, H.; Werner, H. J. *Phys. Chem. Chem. Phys.* **2002**, 4, 1006.
- Pyykkö, P.; Zaleski-Ejgierd, P. J. *Chem. Phys.* **2008**, 128, 124309.
- O'Grady, E.; Kaltsoyannis, N. *Phys. Chem. Chem. Phys.* **2004**, 6, 680.
- Assadollahzadeh, B.; Schwerdtfeger, P. *Chem. Phys. Lett.* **2008**, 462, 222.
- Koch, W.; Holthausen, M. C. *A Chemists' Guide to Density Functional Theory*, 2nd ed.; Wiley–VCH: Weinheim, 2001.
- Dobson, J. F.; McLennan, K.; Rubio, A.; Wang, J.; Gould, T.; Le, H. M.; Dinte, B. P. *Aust. J. Chem.* **2002**, 54, 513.
- Zhao, Y.; Schultz, N. E.; Truhlar, D. G. *J. Chem. Theory Comput.* **2006**, 2, 364.
- Zhao, Y.; Truhlar, D. G. *Theor. Chem. Acc.* **2008**, 120, 215.
- Langreth, D. C.; Lundqvist, B. I.; Chakarova-Kack, S. D.; Cooper, V. R.; Dion, M.; Hyldgaard, P.; Kelkkanen, A.; Kleis, J.; Kong, L.; Li, S.; Moses, P. G.; Murray, E.; Puzder, A.; Rydberg, H.; Schroder, E.; Thonhauser, T. J. *Phys. Condens. Matter* **2009**, 21, 084203.
- Vydrov, O. A.; Voorhis, T. V. J. *Chem. Phys.* **2010**, 132, 164113.
- Grimme, S. *J. Comput. Chem.* **2006**, 27, 1787.
- Grimme, S.; Antony, J.; Ehrlich, S.; Krieg, H. J. *Chem. Phys.* **2010**, 132, 154104.
- Tkatchenko, A.; Scheffler, M. *Phys. Rev. Lett.* **2009**, 102, 073005.
- Becke, A. D.; Johnson, E. R. J. *Chem. Phys.* **2005**, 122, 154104.
- Grimme, S. J. *Chem. Phys.* **2006**, 124, 034108.
- Zhang, Y.; Xu, X.; Goddard, W. A., III. *Proc. Natl. Acad. Sci.* **2009**, 106, 4963.
- Ángyán, J. G.; Gerber, I. C.; Savin, A.; Toulouse, J. *Phys. Rev. A* **2005**, 72, 012510.
- Goll, E.; Werner, H.-J.; Stoll, H. *Chem. Phys.* **2008**, 346, 257.
- Toulouse, J.; Gerber, I. C.; Jansen, G.; Savin, A.; Ángyán, J. G. *Phys. Rev. Lett.* **2009**, 102, 096404.
- Janesko, B. G.; Henderson, T. M.; Scuseria, G. E. J. *Chem. Phys.* **2009**, 130, 081105.
- Goll, E.; Stoll, H.; Thierfelder, C.; Schwerdtfeger, P. *Phys. Rev. A* **2007**, 76, 032507.
- Burns, L. A.; Vázquez-Mayagoitia, Á.; Sumpter, B. G.; Sherrill, C. D. J. *Chem. Phys.* **2011**, 134, 084107.
- Schwerdtfeger, P. *Inorg. Chem.* **1991**, 30, 1660.
- Lieb, E. H.; Oxford, S. *Int. J. Quantum Chem.* **1981**, 19, 427.
- Lacks, D. J.; Gordon, R. G. *Phys. Rev. A* **1993**, 47, 4681.
- Pernal, K.; Podeszwa, R.; Patkowski, K.; Szalewicz, K. *Phys. Rev. Lett.* **2009**, 103, 263201.
- Kannemann, F. O.; Becke, A. D. J. *Chem. Theory Comput.* **2009**, 5, 719.
- Rajchel, L.; Żuchowski, P. S.; Szczesniak, M. M.; Chałasiński, G. *Chem. Phys. Lett.* **2010**, 486, 160.
- Rajchel, L.; Żuchowski, P. S.; Szczesniak, M. M.; Chałasiński, G. *Phys. Rev. Lett.* **2010**, 104, 163001.
- Kamiya, M.; Tsuneda, T.; Hirao, K. J. *Chem. Phys.* **2002**, 117, 6010.
- Figgen, D.; Rauhut, G.; Dolg, M.; Stoll, H. *Chem. Phys.* **2005**, 311, 227.
- Peterson, K. A.; Puzzarini, C. *Theor. Chem. Acc.* **2005**, 114, 283.
- Basis sets were obtained from the Basis Set Exchange Database, Version 1.2.2, as developed and distributed by the Environmental and Molecular Sciences Laboratory which is part of the Pacific Northwest Laboratory, P.O. Box 999, Richland, WA 99352 and funded by the U.S. Department of Energy; see: Feller, D. J. *Comput. Chem.* **1996**, 17, 1571.
- Schuchardt, K. L.; Didier, B. T.; Elsethagen, T.; Sun, L.; Gurumoorthi, V.; Chase, J.; Liand, J.; Windus, T. L. J. *Chem. Inf. Model.* **2007**, 47, 1045.
- Raghavachari, K.; Trucks, G. W.; Pople, J. A.; Head-Gordon, M. *Chem. Phys. Lett.* **1989**, 157, 479.
- Hampel, C.; Peterson, K.; Werner, H.-J. *Chem. Phys. Lett.* **1992**, 190, 1.
- Jeziorski, B.; Moszyński, R.; Szalewicz, K. *Chem. Rev.* **1994**, 94, 1887.
- Żuchowski, P. S.; Busserly-Honvault, B.; Moszynski, R.; Jeziorski, B. J. *Chem. Phys.* **2003**, 119, 10497.
- Jansen, G.; Hesselmann, A. J. *Phys. Chem. A* **2001**, 105, 646.
- Misquitta, A. J.; Szalewicz, K. *Chem. Phys. Lett.* **2002**, 357, 301.
- Werner, H. J.; Knowles, P. J.; Knizia, G.; Manby, F. R.; Schütz, M. et al. *MOLPRO, version 2010.1, a package of ab initio programs*; <http://www.molpro.net> (accessed June 30, 2011).
- Misquitta, A. J.; Jeziorski, B.; Szalewicz, K. *Phys. Rev. Lett.* **2003**, 91, 033201.
- Hesselmann, A.; Jansen, G. *Chem. Phys. Lett.* **2003**, 367, 778.
- Grüning, M.; Gritsenko, O. V.; van Gisbergen, S. J. A.; Baerends, E. J. J. *Chem. Phys.* **2001**, 114, 652.
- Ernzerhof, M.; Scuseria, G. E. J. *Chem. Phys.* **1999**, 110, 5029.
- Adamo, C.; Barone, V. J. *Chem. Phys.* **1999**, 110, 6158.
- Gerber, I. C.; Ángyán, J. G. *Chem. Phys. Lett.* **2005**, 415, 100.
- Vydrov, O. A.; Scuseria, G. E. J. *Chem. Phys.* **2006**, 125, 234109.
- Fromager, E.; Toulouse, J.; Jensen, H. J. A. J. *Chem. Phys.* **2007**, 126, 07411.
- Savin, A. In *Recent developments and Applications of Modern Density Functional Theory*; Seminario, J. M., Ed.; Elsevier: Amsterdam, 1996; pp 327–357.
- Paziani, S.; Moroni, S.; Gori-Giorgi, P.; Bachelet, G. B. *Phys. Rev. B* **2006**, 73, 155111.
- Toulouse, J.; Colonna, F.; Savin, A. J. *Chem. Phys.* **2005**, 122, 14110.
- Goll, E.; Werner, H.-J.; Stoll, H. *Phys. Chem. Chem. Phys.* **2005**, 7, 3917.
- Goll, E.; Werner, H.-J.; Stoll, H.; Leininger, T.; Gori-Giorgi, P.; Savin, A. *Chem. Phys.* **2006**, 329, 276.

- (58) Ernzerhof, M.; Perdew, J. P. *J. Chem. Phys.* **1998**, *109*, 3313.
- (59) Henderson, T. M.; Janesko, B. G.; Scuseria, G. E. *J. Chem. Phys.* **2008**, *128*, 194105.
- (60) Heyd, J.; Scuseria, G. E.; Ernzerhof, M. *J. Chem. Phys.* **2003**, *118*, 8207.
- (61) Huber, K. P.; Herzberg, G. Constants of Diatomic Molecules (data prepared by Gallagher, J. W.; Johnson, R. D., III). In *NIST Chemistry WebBook, NIST Standard Reference Database Number 69*; Linstrom, P. J.; Mallard, W. G., Eds.; National Institute of Standards and Technology: Gaithersburg, MD; <http://webbook.nist.gov> (accessed June 30, 2011).
- (62) Because of the complex's gauche orientation, the monomer geometry has only a minimal effect on the interaction energy of $(\text{HAuPH}_3)_2$. The dispersion energy differs only by 0.07 kcal/mol in the two geometries, and the HF+Disp interaction differs by 0.16 kcal/mol at $R = 3.1\text{\AA}$.
- (63) Danovich, D.; Shaik, S. *J. Chem. Theory Comput.* **2010**, *6*, 1479.
- (64) Misquitta, A. J.; Szalewicz, K. *J. Chem. Phys.* **2005**, *122*, 214109.
- (65) Schwerdtfeger, P.; Bowmaker, G. A. *J. Chem. Phys.* **1994**, *100*, 4487(nonrelativistic). Neogr dy, P.; Kell , V.; Urban, M.; Sadlej, A. J. *Int. J. Quantum Chem.* **1997**, *63*, 557(relativistic).
- (66) Granatier, J.; Urban, M.; Sadlej, A. J. *Chem. Phys. Lett.* **2010**, *484*, 154.
- (67) Pluta, T.; Sadlej, A. J. *Chem. Phys. Lett.* **1998**, *297*, 391.
- (68) Cha asi ski, G.; Szczesniak, M. M.; Kendall, R. A. *J. Chem. Phys.* **1994**, *101*, 8860.
- (69) Klos, J.;  uchowski, P.; Rajchel, L.; Cha asi ski, G.; Szczesniak, M. M. *J. Chem. Phys.* **2009**, *129*, 134302.
- (70) Lee, T. J.; Taylor, P. R. *Int. J. Quant. Chem. Symp.* **1989**, *23*, 199.
- (71) Janssen, C. L.; Nielsen, I. M. B. *Chem. Phys. Lett.* **1998**, *290*, 423.
- Lee, T. J. *Chem. Phys. Lett.* **2003**, *372*, 362.
- (72) Patkowski, K.; Szalewicz, K. *J. Chem. Phys.* **2007**, *127*, 164103.
- (73) <http://www.molpro.net/info/current/doc/manual/node425.html> (accessed June 30, 2011).
- (74) Gutowski, M.; Piel, L. *Mol. Phys.* **1988**, *64*, 337.
- (75) Szabo, A.; Ostlund, N. S. *J. Chem. Phys.* **1977**, *67*, 4351.
- (76) Cha asi ski, G.; Szczesniak, M. M. *Mol. Phys.* **1988**, *63*, 205.
- (77) Gerber, I. C.;  ngy n, J. G. *J. Chem. Phys.* **2007**, *126*, 044103.
- (78) Gerber, I. C.;  ngy n, J. G. *Chem. Phys. Lett.* **2005**, *416*, 370.
- (79) Toulouse, J.; Zhu, W.;  ngy n, J. G.; Savin, A. *Phys. Rev. A* **2010**, *82*, 032502.
- (80) Fromager, E.; Cimraglia, R.; Jensen, H. J. A. *Phys. Rev. A* **2010**, *81*, 024502.
- (81) Janesko, B. G.; Scuseria, G. E. *Phys. Chem. Chem. Phys.* **2009**, *11*, 9677.
- (82) Janesko, B. G.; Henderson, T. M.; Scuseria, G. E. *J. Chem. Phys.* **2009**, *131*, 034110.
- (83) Zhu, W.; Toulouse, J.; Savin, A.;  ngy n, J. G. *J. Chem. Phys.* **2010**, *132*, 244108.
- (84) Riedel, S.; Pyykk , P.; Mata, R. A.; Werner, H. J. *Chem. Phys. Lett.* **2005**, *405*, 148.
- (85) Schwerdtfeger, P.; Bruce, A. E.; Bruce, M. R. M. *J. Am. Chem. Soc.* **1998**, *120*, 6587.

■ NOTE ADDED IN PROOF

The notation for the sr-DFT term should be understood as containing also the long-range HF component.